Strong broadband scattering of anisotropic plasmonic nanoparticles synthesized by controllable growth: effects of lumpy morphology

Xi Chen,[1] Baohua Jia,[1,3] Jhantu Kumar Saha,[1] Nicholas Stokes,[1] Qi Qiao,[2] Yongqian Wang,[2] Zhengrong Shi,[2] and Min Gu[1,*]

[1]*Centre for Micro-Photonics, Faculty of Engineering and Industrial Sciences, Swinburne University of Technology, PO Box 218, Hawthorn, 3122 Victoria, Australia*

[2]*Suntech Power Holdings Co., Ltd., 9 Xinhua Road, New District, Wuxi, Jiangsu Province 214028, China*

[3]*bjia@swin.edu.au*

**mgu@swin.edu.au*

Abstract: Strong scattering intensities in a broadband wavelength range from metallic nanoparticles are essential for diverse photonics applications. Conventional ways of controlling particle scattering are via the control of the size, shape and embedding dielectric environment. In this paper we demonstrate that tailoring the particle surface roughness is another effective way of controlling particle scattering. Roughly surfaced lumpy silver nanoparticles, which have anisotropic surface topography, are realized by a controlled shape- and size-selective wet chemical method. Through the systematic comparison with the smoothly surfaced nanoparticles of the same size and size distribution, we verify both experimentally and theoretically that the lumpy nanoparticles produce large-angle broadband plasmonic scattering due to their unique surface anisotropic structure.

OCIS codes: (160.4236) Nanomaterials; (310.6628) Subwavelength structures, nanostructures; (250.5403) Plasmonics; (040.5350) Photovoltaic.

References and links

1. H. A. Atwater and A. Polman, "Plasmonics for improved photovoltaic devices," Nat. Mater. **9**(3), 205–213 (2010).
2. V. E. Ferry, J. N. Munday, and H. A. Atwater, "Design considerations for plasmonic photovoltaics," Adv. Mater. **22**(43), 4794–4808 (2010).
3. E. Ozbay, "Plasmonics: merging photonics and electronics at nanoscale dimensions," Science **311**(5758), 189–193 (2006).
4. J. N. Anker, W. P. Hall, O. Lyandres, N. C. Shah, J. Zhao, and R. P. Van Duyne, "Biosensing with plasmonic nanosensors," Nat. Mater. **7**(6), 442–453 (2008).
5. F. J. Beck, S. Mokkapati, and K. R. Catchpole, "Light trapping with plasmonic particles: beyond the dipole model," Opt. Express **19**(25), 25230–25241 (2011).
6. F. J. Beck, S. Mokkapati, and K. R. Catchpole, "Plasmonic light-trapping for Si solar cells using self-assembled Ag nanoparticles," Prog. Photovolt. Res. Appl. **18**(7), 500–504 (2010).
7. Z. Ouyang, S. Pillai, F. J. Beck, O. Kunz, S. Varlamov, K. R. Catchpole, P. Campbell, and M. A. Green, "Effective light trapping in polycrystalline silicon thin-film solar cells by means of rear localized surface plasmons," Appl. Phys. Lett. **96**(26), 261109 (2010).
8. N. Fahim, Z. Ouyang, Y. N. Zhang, B. H. Jia, Z. R. Shi, and M. Gu, "Efficiency enhancement of screen-printed multicrystalline silicon solar cells by integrating gold nanoparticles via a dip coating process," Opt. Mater. Express **2**(2), 190–204 (2012).
9. D. M. Schaadt, B. Feng, and E. T. Yu, "Enhanced semiconductor optical absorption via surface plasmon excitation in metal nanoparticles," Appl. Phys. Lett. **86**(6), 063106 (2005).
10. D. Derkacs, S. H. Lim, P. Matheu, W. Mar, and E. T. Yu, "Improved performance of amorphous silicon solar cells via scattering from surface plasmon polaritons in nearby metallic nanoparticles," Appl. Phys. Lett. **89**(9), 093103 (2006).
11. J. L. Wu, F. C. Chen, Y. S. Hsiao, F. C. Chien, P. L. Chen, C. H. Kuo, M. H. Huang, and C. S. Hsu, "Surface plasmonic effects of metallic nanoparticles on the performance of polymer bulk heterojunction solar cells," ACS Nano **5**(2), 959–967 (2011).

#175126 - $15.00 USD Received 28 Aug 2012; revised 9 Dec 2012; accepted 10 Dec 2012; published 11 Dec 2012

12. N. F. Fahim, B. H. Jia, Z. R. Shi, and M. Gu, "Simultaneous broadband light trapping and fill factor enhancement in crystalline silicon solar cells induced by Ag nanoparticles and nanoshells," Opt. Express **20**(S5 Suppl 5), A694–A705 (2012).
13. Y. N. Zhang, Z. Ouyang, N. Stokes, B. H. Jia, Z. R. Shi, and M. Gu, "Low cost and high performance Al nanoparticles for broadband light trapping in Si wafer solar cells," Appl. Phys. Lett. **100**(15), 151101 (2012).
14. X. Chen, B. H. Jia, J. K. Saha, B. Y. Cai, N. Stokes, Q. Qiao, Y. Q. Wang, Z. R. Shi, and M. Gu, "Broadband enhancement in thin-film amorphous silicon solar cells enabled by nucleated silver nanoparticles," Nano Lett. **12**(5), 2187–2192 (2012).
15. J. P. Singh, T. E. Lanier, H. Zhu, W. M. Dennis, R. A. Tripp, and Y. P. Zhao, "Highly sensitive and transparent surface enhanced Raman scattering substrates made by active coldly condensed Ag nanorod arrays," J. Phys. Chem. C **116**(38), 20550–20557 (2012).
16. Q. Zhou, Y. P. He, J. Abell, Z. J. Zhang, and Y. P. Zhao, "Optical properties and surface enhanced Raman scattering of L-shaped silver nanorod arrays," J. Phys. Chem. C **115**(29), 14131–14140 (2011).
17. N. R. Jana, "Gram-scale synthesis of soluble, near-monodisperse gold nanorods and other anisotropic nanoparticles," Small **1**(8-9), 875–882 (2005).
18. N. R. Jana, L. Gearheart, and C. J. Murphy, "Wet chemical synthesis of high aspect ratio cylindrical gold nanorods," J. Phys. Chem. B **105**(19), 4065–4067 (2001).
19. D. Zhang, L. Qi, J. Yang, J. Ma, H. Cheng, and L. Huang, "Wet chemical synthesis of silver nanowire thin films at ambient temperature," Chem. Mater. **16**(5), 872–876 (2004).
20. M. J. Mulvihill, X. Y. Ling, J. Henzie, and P. D. Yang, "Anisotropic etching of silver nanoparticles for plasmonic structures capable of single-particle SERS," J. Am. Chem. Soc. **132**(1), 268–274 (2010).
21. P. Zijlstra, J. W. M. Chon, and M. Gu, "Five-dimensional optical recording mediated by surface plasmons in gold nanorods," Nature **459**(7245), 410–413 (2009).
22. Y. A. Akimov, W. S. Koh, and K. Ostrikov, "Enhancement of optical absorption in thin-film solar cells through the excitation of higher-order nanoparticle plasmon modes," Opt. Express **17**(12), 10195–10205 (2009).
23. Lumerical, "FDTD solutions" (Lumerical, Toronto, Canada, accessed August 2012), http://www.lumerical.com/tcad-products/fdtd/.
24. E. Moulin, J. Sukmanowski, P. Luo, R. Carius, F. Royer, and H. Stiebig, "Improved light absorption in thin-film silicon solar cells by integration of silver nanoparticles," J. Non-Cryst. Solids **354**(19-25), 2488–2491 (2008).
25. K. R. Catchpole and A. Polman, "Design principles for particle plasmon enhanced solar cells," Appl. Phys. Lett. **93**(19), 191113 (2008).
26. C. Hägglund, M. Zach, G. Petersson, and B. Kasemo, "Electromagnetic coupling of light into a silicon solar cell by nanodisk plasmons," Appl. Phys. Lett. **92**(5), 053110 (2008).
27. D. Duche, P. Torchio, L. Escoubas, F. Monestier, J. J. Simon, F. Flory, and G. Mathian, "Improving light absorption in organic solar cells by plasmonic contribution," Sol. Energy Mater. Sol. Cells **93**(8), 1377–1382 (2009).
28. S. Pillai, K. R. Catchpole, T. Trupke, and M. A. Green, "Surface plasmon enhanced silicon solar cells," J. Appl. Phys. **101**(9), 093105 (2007).

1. Introduction

Plasmonic light scattering from metallic nanostructures has demonstrated a great potential in diverse applications such as photovoltaics [1,2], nanophotonics [3] and biochemical sensing [4]. Among the various reported plasmonic nanostructures, metallic nanoparticles are the simplest, cheapest and most mass-producible candidate holding a great promise for future large-scale applications [5–11]. The last several years have witnessed an explosion of interest in investigating the plasmonic resonance enhanced scattering properties of metallic nanoparticles [5–14]. Scattering intensity, operational bandwidths and scattering angles are three key metrics for the evaluation of the light scattering effect.

Conventional ways of controlling the nanoparticle scattering rely on controlling the particle shapes, sizes, size distribution statistics and their embedding dielectric environments [1]. However there is a great challenge to achieve a high scattering strength over a board wavelength range as well as a large angular range in terms of the conventional method. Limited spectral broadening has been observed with unintentionally induced size or shape non-uniformities and therefore little control has been realized in the broadband light scattering [10]. In this paper we demonstrate that engineering the nanoparticle surface topography to form a kind of lumpy nanoparticles, which consists of a large core particle with surrounding small nanoparticles, is an effective way to achieve this goal. Roughly surfaced nanoparticles have been utilized to improve the scattering intensity for thin film solar cells and surface-enhanced Raman spectroscopic applications [14–16], however no research has been carried out to identify the key parameters that can facilitate the maximization of the broadband scattering strength. Fundamentally, achieving a controllable growth of the anisotropic lumpy

#175126 - $15.00 USD Received 28 Aug 2012; revised 9 Dec 2012; accepted 10 Dec 2012; published 11 Dec 2012

nanoparticles is yet revealed. Here the controllable growth of the lumpy nanoparticles with different morphologies is achieved by adjusting the reductants and solution viscosities with a modified wet chemical method. The scattering effect of the lumpy nanoparticles is then systematically compared with that of the smoothly surfaced nanoparticles with the same sizes and size distributions. The finite difference time domain (FDTD) simulations consistently confirm that the anisotropic lumpy nanoparticles possess a broadband light scattering capability with scattering intensities and scattering angles higher than those of the smoothly surfaced nanoparticles. Finally, the identified key parameters of growth-controlled lumpy nanoparticles are applied to photovoltaic devices, which show an overall short circuit current density (J_{sc}) enhancement.

2. Controllable synthesis of lumpy anisotropic silver nanoparticles

To realize the lumpy nanoparticles, the particle size and shape need to be controlled simultaneously during the crystal growth. It is challenging to use the conventional reduction method with strong reductant to produce the lumpy nanoparticles because it induces rapid nucleation leading only to smoothly surfaced nanoparticles [17]. To solve this problem, the wet chemical method was modified to be shape-selective with a milder reducing agent - ascorbic acid was used for the reduction of the silver ions in this paper [17–19]. First, 0.1 mmol ascorbic acid was added into 5 ml of solution with different concentrations of polyvinyl alcohol (PVA). Next, 0.5 ml of 0.2 M $AgNO_3$ was injected drop wise with shaking. The solution was centrifuged and then the precipitate, containing the silver lumpy nanoparticles, was redispersed into de-ionized water. For comparison, smoothly surfaced silver nanoparticles were synthesized with an identical process except that the reductant was $NaBH_4$.

The morphology of the growth-controlled silver nanoparticles was characterized by a scanning electron microscope (SEM) system (ZEISS Supra 40). SEM image of the as-prepared anisotropic silver particles under a PVA concentration of 3 g/l is shown in Fig. 1(b). Obviously the particles present large surface roughness mimicking the lumpy model with both a large core particle and the small surface particles, presented in Fig. 1(a). The sizes of the small surface particles approximately occupy 1/4 to 1/2 of the core size. We believe that the shape-selective crystal growth of the nanoparticles is a result of the direction-dependent agglomeration. In our study a weaker reducing agent-ascorbic acid rather than $NaBH_4$ is used for the formation of silver atoms slowly from the silver ions, causing the anisotropic growth from certain crystalline bounds [17]. We suggest that the growth of the anisotropic particle proceed in both {100} and {111} bounds, because this kind of the structure demonstrates an

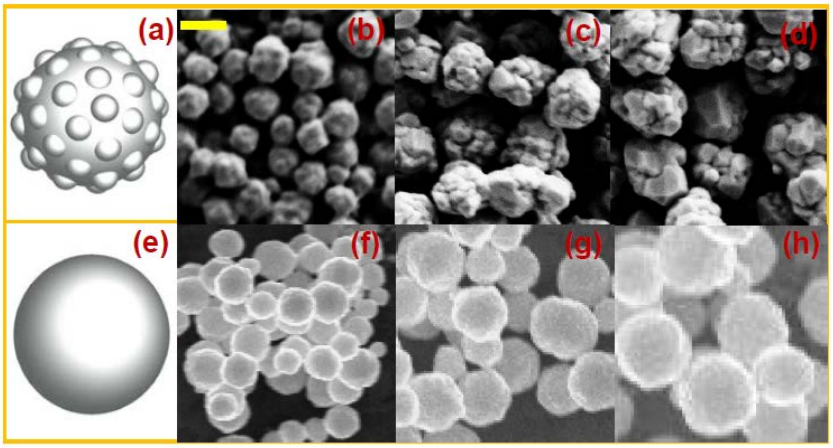

Fig. 1. (a) Schematic drawing of a lumpy nanoparticle. (b-d) SEM images of the lumpy silver nanoparticles with diameters of (b) 150 nm, (c) 200 nm and (d) 250 nm. (e) Schematic drawing of a smoothly surfaced nanoparticle. (f-h) SEM images of the smoothly surfaced silver nanoparticles with diameters of (f) 150 nm, (g) 200 nm and (h) 250 nm. Scale bar: 200 nm.

#175126 - $15.00 USD Received 28 Aug 2012; revised 9 Dec 2012; accepted 10 Dec 2012; published 11 Dec 2012

intermediate morphology between the {100}-bound cube and {111}-bound octahedral [20]. In comparison the silver nanoparticles synthesized with $NaBH_4$ reductant present smooth surfaces and spherical shapes, as shown in Figs. 1(e)-1(h).

Moreover, the size of the as-prepared silver nanoparticles can be tailored by adjusting the nucleation rate via changing the PVA concentrations, since the viscosity of the reaction solution is determined by the PVA addition [17]. In Figs. 1(b)-1(d) and 1(f)-1(h), both the lumpy and the smoothly surfaced nanoparticles with diameters of 150 nm, 200 nm and 250 nm were synthesized by PVA concentrations of 1 g/l, 3 g/l and 5 g/l, respectively.

The size distributions of the anisotropic lumpy and the smoothly surfaced nanoparticles are shown in Fig. 2. To eliminate the possible spectral broadening resulted from the size and size distribution of the nanoparticles, the synthesis process was carefully controlled by the utilization of the optimized PVA concentration and stirring intensity. The aim in the controlling process is to allow the same sized lumpy and smoothly surfaced nanoparticles to have the similar distribution statistics, as shown in Fig. 2.

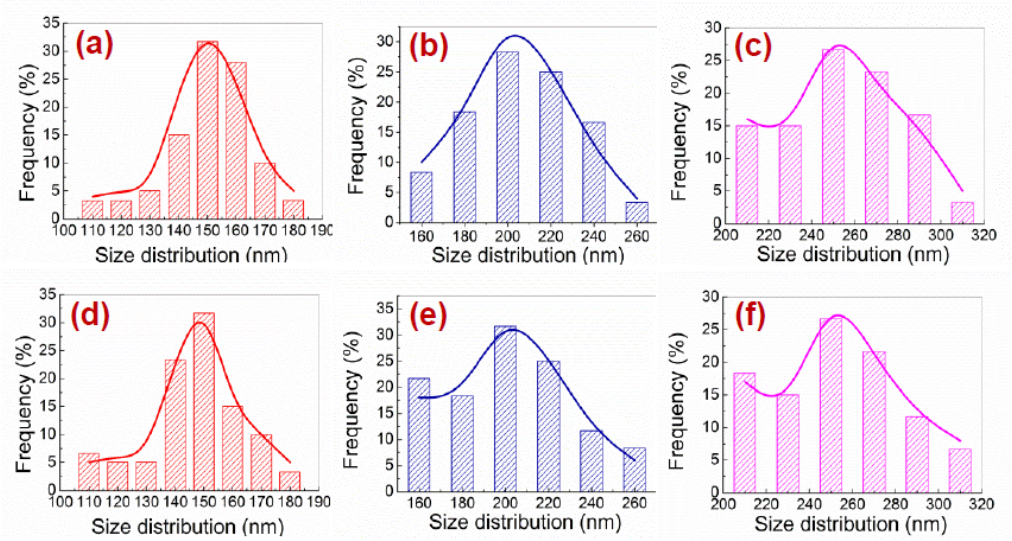

Fig. 2. Size distribution graphs of (a-c) 150 nm, 200 nm and 250 nm lumpy silver nanoparticles, respectively, and (d-f) 150 nm, 200 nm and 250 nm smoothly surfaced silver nanoparticles, respectively.

3. Plasmonic scattering properties of lumpy silver nanoparticles

The comparison of the extinction spectra of the lumpy and smoothly surfaced nanoparticles is shown in Fig. 3. For smoothly surfaced nanoparticles, obvious narrow-band plasmonic resonance peaks can be seen at 457 nm, 597 nm and 745 nm for nanoparticles with diameters of 150 nm, 200 nm and 250 nm, respectively. The resonance peaks shift to the longer wavelengths with increased nanoparticle size and become broadened with increased size distribution. In contrast, all the lumpy nanoparticles exhibit broadband plasmonic features within the interested wavelength range (300 to 800 nm) independent on the particle size and size distribution. Such a unique broadband feature is a direct result of the novel anisotropic particle hierarchy with both the large core particles and the small surface particles, which allows the excitation of the multiple resonance modes in a wide range of the wavelength [21,22].

In Figs. 4(a) and 4(b) the far-field scattering intensity mappings of 200 nm smoothly surfaced and lumpy nanoparticles as a function of the scattering angle and the incident unpolarized solar spectrum are presented. It is clear that for both particles most light undergoes forward scattering (the incident direction is along 180°). However, the scattering

#175126 - $15.00 USD Received 28 Aug 2012; revised 9 Dec 2012; accepted 10 Dec 2012; published 11 Dec 2012

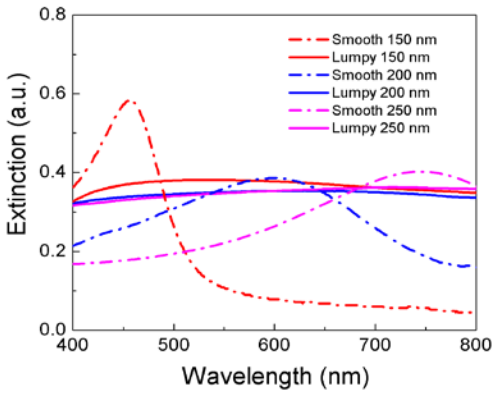

Fig. 3. Measured UV-visible extinction spectra of silver lumpy (solid) and smoothly surfaced (dash dot) nanoparticle suspension with different diameters of 150 nm (red), 200 nm (blue), and 250 nm (magenta), respectively. Each extinction spectrum is averaged from three measurements. The measurement error is estimated to be within ±1%.

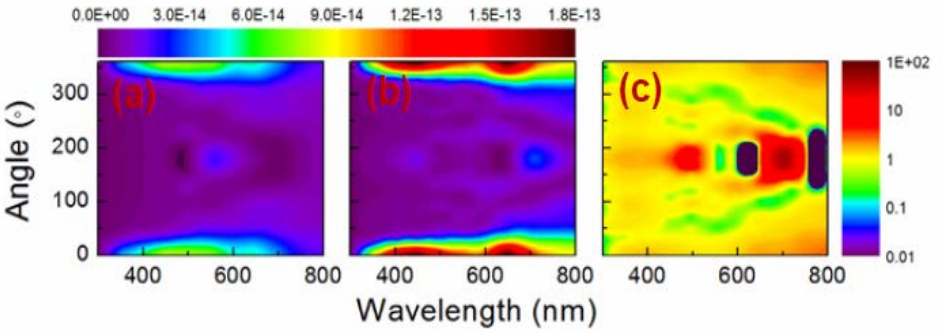

Fig. 4. FDTD simulation of the scattering intensity mappings as a function of the scattering angle and the incident wavelength of a 200 nm (a) smoothly surfaced nanoparticle; (b) lumpy nanoparticle; (c) the scattering enhancement mapping by dividing (a) by (b).

angle of the lumpy nanoparticles is much wider than that of the smoothly surfaced nanoparticles. More importantly, broadband scattering is achieved for the lumpy nanoparticles from 300 nm to 800 nm when the scattering angles are close to 360° with a peak scattering intensity of the lumpy nanoparticle almost three times of that of the smoothly surfaced nanoparticle. To better compare the scattering capability, in Fig. 4(c) the mapping of the scattering intensity of the lumpy nanoparticle is normalized to that of the smoothly surfaced nanoparticle. It can be seen that for almost all of the angles and wavelengths the lumpy nanoparticle outperforms the smoothly surfaced nanoparticle. In particular, apart from the dominate forward scattering, the lumpy nanoparticle can also induce strong broadband back scattering from 300 nm to 510 nm and from 620 nm to 760 nm with a peak intensity almost two orders of magnitude higher than that of the smoothly surfaced nanoparticles. However, from 510 to 620 nm, the backward scatterings of these two cases are quite comparable. The results undoubtedly convince that tailoring the plasmonic particle surface roughness can maximize the large-angle broadband scattering strength.

4. Photovoltaic applications of lumpy silver nanoscatterers

Due to the superior plasmonic scattering properties, the silver lumpy nanoparticle manifests attractive potential applications in photonic devices. Here we provide an example of using the identified key parameters of growth-controlled nanoparticles in the plasmonic photovoltaic devices. When being integrated into the rear-side ZnO:Al layer of the thin-film amorphous

#175126 - $15.00 USD Received 28 Aug 2012; revised 9 Dec 2012; accepted 10 Dec 2012; published 11 Dec 2012

silicon solar cells, such lumpy nanoparticles are expected to scatter the incident light into a large angle much more strongly over a broad wavelength range than the smoothly surfaced particles. To examine the superior scattering effect of the lumpy nanoparticles, FDTD simulation [23] was conducted to compare the scattering cross-sections of the lumpy and smoothly surfaced nanoparticles of the same sizes. The details of the modeling are provided in Ref 14 and the results are shown in Fig. 5. Since the nanoparticles were integrated at the back of the solar cells, sunlight before 530 nm was sufficiently absorbed by the cells [14]. Only the wavelength range from 530 to 800 nm was plotted in Fig. 5. The lumpy particles show a scattering peak around 660 nm due to the plasmon resonance of the large core particle, and another peak around 550 nm from the surface roughness. It can be clearly seen that the scattering cross-sections increase with particle sizes. For all the three investigated sizes, the lumpy nanoparticles exhibit much larger scattering cross-sections over a broad wavelength range than those of the smoothly surfaced nanoparticles. The scattering cross-section of the 200 nm lumpy nanoparticle is even larger than that of the smoothly surfaced nanoparticle with 250 nm in size from 620 to 800 nm. The wavelength integrated scattering cross-sections from 530 nm to 800 nm of 150, 200 and 250 nm lumpy nanoparticles are greater than their smoothly surfaced counterparts by 45%, 63% and 35%, respectively, suggesting that the 200 nm lumpy nanoparticles can potentially induce the largest enhancement compared to the smoothly surfaced nanoparticles in the light scattering effect in solar cells.

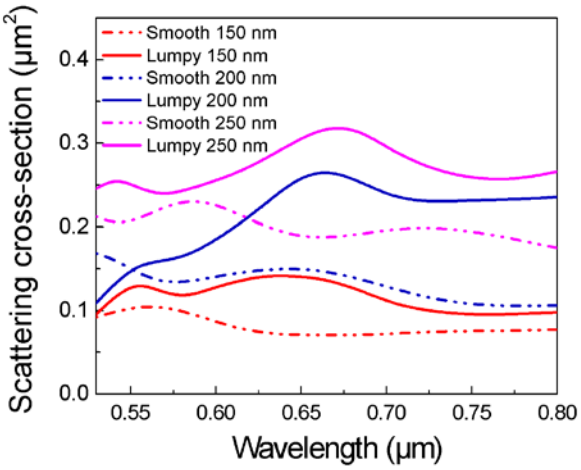

Fig. 5. Calculated scattering cross-sections for lumpy and smoothly surfaced nanoparticles with diameters of 150 nm, 200 nm and 250 nm in a ZnO:Al layer.

To further confirm the light scattering properties of the lumpy nanoparticles experimentally, we integrated them into the rear side of amorphous silicon thin-film solar cells. The integration procedure of the particle is shown in the inset of Fig. 6. Before the integration of the nanoparticles, the surfaces of the thin-film solar cells (without the back contacts) were cleaned in ethanol solution under sonication. Next, silver nanoparticles were integrated onto the rear-side ZnO:Al layer by the deposition of the nanoparticle aqueous suspension at an optimize surface coverage of 10% [14]. The ZnO:Al layer thickness between the nanoparticles and the silicon layer (350 nm in total) was 20 nm. Finally another ZnO:Al layer and the silver back contact were sputtered on top of the nanoparticles in order to embed the particles into the ZnO:Al layer.

The comparison of the J_{sc} enhancements of the solar cells integrated with different sized lumpy and smoothly surfaced nanoparticles normalized to those without nanoparticles is presented in Fig. 6. Due to the enhanced light scattering, both the lumpy and the smoothly surfaced nanoparticles increase the optical path length in the amorphous silicon layer and thereby increase J_{sc} of the solar cells as shown in Fig. 6, in which J_{sc} enhancement is achieved

#175126 - $15.00 USD Received 28 Aug 2012; revised 9 Dec 2012; accepted 10 Dec 2012; published 11 Dec 2012

in all cases. However, the enhancement from the lumpy nanoparticles is remarkably and consistently higher than that from the smoothly surfaced nanoparticles of all three sizes. The largest J_{sc} enhancement can be achieved for the 200 nm lumpy nanoparticles matching the predication of our FDTD simulation shown in Fig. 5. A 14.3% increase in J_{sc} is realized in this case, while for the smoothly surfaced nanoparticles with the identical diameters, only 8.3% J_{sc} enhancement can be observed. In terms of the solar cells integrated with the 150 nm silver nanoparticles, under the same experimental conditions lower J_{sc} enhancements are achieved compared with those integrated with the 200 nm nanoparticles because of the relatively smaller scattering cross-sections [24–28]. The J_{sc} enhancement by around 11.4% and 7.5% for the lumpy and smoothly surfaced particle integrated solar cells can be realized, respectively. Different from the simulation predication in Fig. 5, the absolute J_{sc} enhancement induced by the 250 nm particles is smaller than that induced by the 200 nm nanoparticles for both the lumpy and smoothly surfaced nanoparticle cases. This is possibly due to two reasons. First of all, although the scattering cross-section is larger, the coupling of the scattered light to the silicon absorbing layer might not be efficient due to the excitation of the higher-order plasmonic modes [22]. Secondly, due to the larger size of the nanoparticle, it might cause some contact loss at the back reflector. The enhancement difference between the lumpy and smoothly surfaced nanoparticles is the smallest for the 250 nm nanoparticles, which qualitatively agrees with the simulation predications in Fig. 5. The results in Fig. 6 have unambiguously demonstrated that the growth-controlled lumpy nanoparticles can induce superior broadband light scattering, leading to a dramatic solar cell performance improvement.

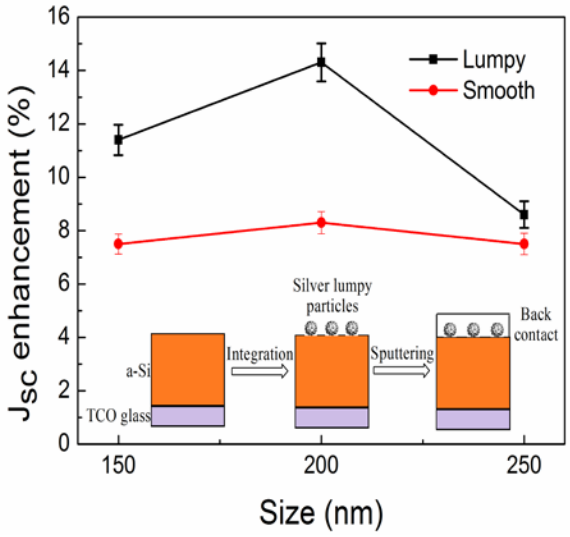

Fig. 6. J_{sc} enhancements of thin-film amorphous silicon solar cells integrated with silver lumpy nanoparticles and smoothly surfaced nanoparticles with the same size and size distribution. Inset: schematic drawings of the lumpy silver particle integration into the ZnO:Al layer of the amorphous silicon solar cells.

5. Conclusion

In conclusion, growth-controlled anisotropic silver nanoparticles have been achieved by a unique shape- and size-selective wet chemical method. The effectiveness of the lumpy-shaped nanoparticles in plasmonic light scattering has been examined both theoretically and experimentally by the systematic comparison with smoothly surfaced nanoparticles of the same sizes and size distributions. The comparisons of the scattering cross-sections and scattering angles have consistently demonstrated that the innovative lumpy nanoparticles can

#175126 - $15.00 USD Received 28 Aug 2012; revised 9 Dec 2012; accepted 10 Dec 2012; published 11 Dec 2012

much more effectively scatter light in a broad spectral range with a large scattering angle. The lumpy nanoparticle provides a new strategy of engineering the particle surface roughness to realize large-angle broadband light scattering for diverse applications including photovoltaics, nanophotonics and biochemical sensing.

Acknowledgments

The authors acknowledge the financial support from the Victorian Government to establish the Victoria-Suntech Advanced Solar Facility (VSASF) under the Victoria Science Agenda (VSA) scheme. B.J. thanks the Victorian Government for the support through the Victorian Fellowship and L´Oréal through the L´Oréal Australia and New Zealand For Women in Science Fellowship.

#175126 - $15.00 USD Received 28 Aug 2012; revised 9 Dec 2012; accepted 10 Dec 2012; published 11 Dec 2012